

# Fast and accurate emulation of complex dynamic simulators

Junoh Heo

Michigan State University

## Abstract

While dynamic simulators, which are computational models that evolve over time and are governed by differential equations, are essential in scientific and engineering applications, their emulation remains challenging due to the unpredictable behavior of complex systems. To address this challenge, this paper introduces a fast and accurate Gaussian Process (GP)-based emulation method for complex dynamic simulators. By integrating linked GPs into the one-step-ahead emulation framework, the proposed algorithm enables exact analytical computations of the posterior mean and variance, eliminating the need for computationally expensive Monte Carlo approximations. This significantly reduces computation time while maintaining or improving predictive accuracy. Furthermore, the method extends naturally to systems with forcing inputs by incorporating them as additional variables within the GP framework. Numerical experiments on the Lotka-Volterra model and the Lorenz system demonstrate the efficiency and computational advantages of the proposed approach. An R package, *dynemu*, implementing the one-step-ahead emulation approach, is available on CRAN.

*Keywords:* Surrogate model, Linked Gaussian processes, Complex system, Uncertainty propagation

# 1 Introduction

Computer models, often referred to as computer simulators, are indispensable tools for simulating complex systems and processes to gain insights into physical or scientific phenomena. Many of these models evolve over time and are governed by intricate systems of differential equations, collectively known as dynamic simulators (Scheinerman, 2012). Dynamic simulators are used to describe a wide range of phenomena across diverse fields, including meteorology (Millán et al., 2009), hydrology (Li et al., 2016), physics (Bahamonde et al., 2018), engineering (Bongard and Lipson, 2007), and biology (Hwang et al., 2025), among others. These models are particularly crucial for studying problems where analytical solutions to the governing equations are either impractical or infeasible.

Dynamic systems often have *forcing inputs*, which are external or time-varying variables that influence the system’s evolution. Examples include external forces in mechanical systems, atmospheric conditions in climate models, or control inputs in engineering applications. These inputs are typically included as additional input variables in the emulator and are usually assumed to be known. Their presence modifies the system dynamics, necessitating an adaptation of the emulation approach to capture their effects properly.

Despite their utility, dynamic simulators often come with significant computational demands, which can limit their practicality in certain applications. These models typically require solving systems of ordinary differential equations (ODEs), which can be computationally intensive, especially when simulations must be repeated for tasks such as optimization, sensitivity analysis, or uncertainty quantification. To overcome these limitations, emulation offers an efficient alternative by constructing surrogate models that approximate the behavior of the simulator. Surrogate models emulate the simulator’s outputs at a fraction of the computational cost, enabling researchers to conduct extensive analyses without the

prohibitive expense of repeated direct simulations. This capability enhances the utility of dynamic simulators, facilitating faster and more scalable solutions to complex problems across scientific and engineering domains.

GPs (Rasmussen and Williams, 2006) are a widely used choice for constructing emulators due to their flexibility, accuracy, and strong theoretical foundation. They are particularly well-suited for approximating the complex, non-linear relationships commonly encountered in real-world problems. A key advantage of GPs lies in their ability not only to provide mean predictions but also to quantify uncertainty through analytical expressions of posteriors. Moreover, GPs naturally interpolate training data, ensuring exact predictions at observed points. This interpolation property is particularly important for dynamic simulators, which are inherently deterministic, as it preserves the consistency of the emulator with the original simulator outputs.

Several GP emulators for dynamic simulators have been developed, ranging from classic methods to recent advancements (Girard et al., 2002; Bhattacharya, 2007; Conti et al., 2009; Mohammadi et al., 2024), achieving significant performance improvements. For a detailed overview of dynamic simulator emulation, we refer readers to Mohammadi et al. (2024). Notably, Bhattacharya (2007) proposed a one-step-ahead emulation approach, which assumes that the model output at time  $t$  depends only on the output at the previous time point  $t - 1$ , a property commonly referred to as the Markov property. Building on this, Mohammadi et al. (2019) enhanced the approach by incorporating input uncertainty and emulating the numerical flow map. Despite these advancements, many emulators still require intensive computations, such as Monte Carlo (MC) approximations (Conti et al., 2009; Mohammadi et al., 2019) or grid-based methods (Bhattacharya, 2007).

To the best of our knowledge, the posterior distribution of GPs with uncertain inputs is known to be intractable, necessitating the use of MC methods (Girard et al., 2002;

Mohammadi et al., 2019) in the context of dynamic simulators. To address this limitation, Mohammadi et al. (2024) recently employed random Fourier features to approximate the kernel. However, maintaining the quality of the approximated kernel requires drawing hundreds of random features. Furthermore, generating predictions involves drawing hundreds of additional sample paths from the emulated flow map. These computational demands may limit the practical advantages of emulators, highlighting the need for more efficient approaches.

In this article, we propose a fast and more accurate emulation method for dynamic simulators by treating the emulator as self-coupled, adopting the one-step-ahead approach while overcoming the aforementioned limitations of MC approximations. The proposed method builds on the framework of Mohammadi et al. (2019) but replaces the approximated distribution with the exact mean and variance. These analytically tractable predictive posterior mean and variance, enabled by Linked GPs (Kozyurova et al., 2018; Ming and Guillas, 2021), facilitate the computation of exact posteriors, thus eliminating the need for time-consuming MC approximations. Linked GPs, originally developed for coupled computer models, allow for the analytical derivation of the mean and variance of GPs at random inputs. These closed-form expressions are achievable with commonly used kernels, such as the squared exponential kernel or the Matérn kernel (Stein, 1999), with smoothness parameters  $\nu = 1.5$  and  $\nu = 2.5$ . By leveraging this framework, the proposed model achieves computational efficiency without any loss of information, as the computational burdens of most existing methods primarily arise from the approximation step.

The remainder of this article is organized as follows. Section 2 provides a review of GP emulators, linked GPs, and the one-step-ahead approach. The proposed fast and accurate emulation method is introduced in Section 3. Section 4, presents several numerical studies to demonstrate the competitiveness of the proposed method. Finally, Section 5 concludes

the paper.

## 2 Review

### 2.1 Gaussian processes

Let  $f : \mathbb{R}^d \rightarrow \mathbb{R}$  represent the computer code output as a deterministic black-box function of the input  $\mathbf{x}$ , where  $\mathbf{x} \in \mathcal{X} \subseteq \mathbb{R}^d$ , and the corresponding output is  $y = f(\mathbf{x})$ . Typically, a GP prior assumes that the simulation outputs  $\mathbf{y}$  follow a multivariate normal distribution:

$$\mathbf{y} \sim \mathcal{N}(\alpha(\mathbf{x}), \tau^2 K(\mathbf{x}, \mathbf{x}')),$$

where  $\alpha(\mathbf{x})$  is the mean function,  $\tau^2$  is a scale parameter, and  $K(\mathbf{x}, \mathbf{x}')$  is a positive-definite kernel matrix. Popular choices for the mean function  $\alpha(\mathbf{x})$  include linear  $(1, \mathbf{x}^T)\beta$ , constant  $\alpha$ , or zero, where  $\beta$  is a vector of  $d + 1$  regression coefficients. For the kernel  $K$ , the squared exponential kernel or Matérn kernel is commonly adopted. In this paper, we focus on the anisotropic squared exponential kernel  $K(\mathbf{x}, \mathbf{x}') = \exp\left(-\sum_{k=1}^d \frac{(x_k - x'_k)^2}{\theta_k}\right)$ , where  $(\theta_1, \dots, \theta_d)$  are the lengthscales hyperparameters that represent the rate of decay of correlation in each input dimension.

The posterior prediction of GPs at a new input point  $\mathbf{x}$ , given the input design  $X = (\mathbf{x}_1, \dots, \mathbf{x}_n) \subset \mathbb{R}^{n \times d}$  and corresponding outputs  $\mathbf{y}$ , is given as:

$$\begin{aligned} \mu(\mathbf{x}) &= \alpha(\mathbf{x}) + \mathbf{k}^T(\mathbf{x})\mathbf{K}^{-1}(\mathbf{y} - \alpha(X)), \quad \text{and} \\ \sigma^2(\mathbf{x}) &= \tau^2 (1 - \mathbf{k}^T(\mathbf{x})\mathbf{K}^{-1}\mathbf{k}(\mathbf{x})), \end{aligned}$$

where  $\mathbf{k}(\mathbf{x})_i = K(X, \mathbf{x})_i$  and  $\mathbf{K}_{ij} = K(\mathbf{x}_i, \mathbf{x}_j)$ . For more details about GPs in the context of

computer experiments, we refer to Santner et al. (2018) and Gramacy (2020).

The parameters  $\{\beta, \tau^2, \theta_1, \dots, \theta_d\}$  in the GP model can be estimated by maximizing the log-likelihood:

$$-\frac{1}{2} \left( n \log 2\pi + n \log \tau^2 + \log |\mathbf{K}| + \frac{1}{\tau^2} (\mathbf{y} - \alpha(X))^T \mathbf{K}^{-1} (\mathbf{y} - \alpha(X)) \right).$$

The profile log-likelihood is obtained by substituting the analytical expressions of  $\hat{\beta}$  and  $\hat{\tau}^2$ :

$$\hat{\beta} = (X_n^T \mathbf{K}^{-1} X_n)^{-1} X_n^T \mathbf{K}^{-1} \mathbf{y} \quad \text{and} \quad \hat{\tau}^2 = \frac{(\mathbf{y} - (1, X_n^T) \hat{\beta})^T \mathbf{K}^{-1} (\mathbf{y} - (1, X_n^T) \hat{\beta})}{n}.$$

In practice, optimization algorithms such as L-BFGS-B (Byrd et al., 1995; Zhu et al., 1997) are commonly employed to maximize the log-likelihood.

## 2.2 Linked GPs

Linked GP emulators (Kyzyurova et al., 2018; Ming and Guillas, 2021) are designed to emulate two or more coupled systems of computer models. Consider  $n_1$  computer models at the first layer,  $f_l : \mathbb{R}^{d_1} \rightarrow \mathbb{R}$  for  $l = 1, \dots, n_1$ , which are connected to a second-layer model  $g : \mathbb{R}^{d_2} \rightarrow \mathbb{R}$ . In this framework, the outputs of  $f_1, \dots, f_{n_1}$  serve as part of the input to  $g$ . Assuming that  $f_1, \dots, f_{n_1}$  are independent and share the same set of inputs, the posterior predictive distribution at a new input  $\mathbf{x}$ , given the input-output pairs  $(X_n, f_l(X_n))_{l=1, \dots, n_1}$

and  $(Z_n, g(Z_n))$  is expressed as:

$$\begin{aligned}
& p(g \circ (f_1, \dots, f_{n_1})(\mathbf{x}) | \{f_l(X_n)\}_{l=1, \dots, n_1}, g(Z_n), \mathbf{x}) \\
&= \int p(g(\mathbf{x}_g, f_1(\mathbf{x}_f), \dots, f_{n_1}(\mathbf{x}_f)) | \{f_l(X_n)\}_{l=1, \dots, n_1}, g(Z_n), \mathbf{x}) \\
&\quad \times \prod_{l=1}^{n_1} p(f_l(\mathbf{x}_f) | f_l(X_l)) df_1(\mathbf{x}_f) \dots df_{n_1}(\mathbf{x}_f)
\end{aligned} \tag{1}$$

where  $\mathbf{x}_g$  denotes the unlinked inputs of  $g$ , and  $\mathbf{x}_f$  represents the inputs for  $f_1, \dots, f_{n_1}$ , which are a subset of  $\mathbf{x}$ . This posterior is known to be analytically intractable (Girard et al., 2002). Numerical techniques, such as Markov Chain Monte Carlo, can approximate the posterior but are computationally demanding. To address this limitation, subsequent works replaced  $f_1, \dots, f_{n_1}$  and  $g$  with their respective GP emulators  $\hat{f}_1, \dots, \hat{f}_{n_1}$  and  $\hat{g}$  and applied Gaussian approximations. Using this approach, Kyzyurova et al. (2018) derived the closed-form expressions under the squared exponential kernel, and Ming and Guillas (2021) extended the posterior to the Matérn kernels.

Linked GP emulators minimize the Kullback-Leibler divergence between the emulator and a Gaussian density (Ming and Guillas, 2021). Moreover, they demonstrate superior performance compared to composite emulator, which disregard the coupled relationships and consider only the inputs of the first layer and the outputs of the final layer. This concept of linked GPs can be naturally extended to systems with multiple layers involving iterative or parallel structures (Ming and Guillas, 2021; Heo and Sung, 2023), high-dimensional output (Dolski et al., 2024), as well as deep GPs (Ming et al., 2023).

### 2.3 One-step-ahead emulations

Consider a dynamic computer simulator without forcing input  $f : \mathbb{R}^d \rightarrow \mathbb{R}^{d \times T}$  that produces  $T$  outputs evolving over time. The simulator  $f$  is governed by  $d$  ODEs, where the state variables at time  $t_s$  are expressed as  $\mathbf{x}(t_s) = (x_1(t_s), \dots, x_d(t_s))^T$ , for  $s = 0, \dots, T$ . The one-step-ahead approach emulates the system’s flow map over short time intervals, assuming the Markov property, which states that the state  $\mathbf{x}(t_s)$  depends only on the previous state  $\mathbf{x}(t_{s-1})$ . Once an emulator  $\hat{f}$  is constructed based on the input-output pairs at the initial condition  $\mathbf{x}(t_0)$  and the corresponding output  $\mathbf{x}(t_1)$ , predictions for future states  $\hat{\mathbf{x}}(t_s)$  for  $s = 1, \dots, T$  can be obtained iteratively by leveraging the Markov assumption (Mohammadi et al., 2019, 2024):

$$\hat{x}_m(t_{s+1}) = \hat{f}_m(\mathbf{x}(t_s)), \quad (2)$$

where  $m = 1, \dots, d$ . This approach is particularly effective for periodic systems, as it can accurately predict the next state based on the current state within the input range, making it ideal for capturing the system’s repetitive dynamics. Furthermore, the one-step-ahead approach provides an efficient, reliable, and computationally inexpensive alternative to other emulation methods for dynamic simulators (Conti et al., 2009; Stolfi and Castiglione, 2021).

Mohammadi et al. (2019) incorporate input uncertainty at each time step into the emulators by adopting MC methods and leveraging the laws of total expectation and total



variance to approximate the posterior in (1):

$$\mathbb{E}[\hat{x}_m(t_s)] = \mathbb{E}[\hat{f}_m(\mathbf{x}(t_{s-1}))] = \mathbb{E}\left[\mathbb{E}[\hat{f}_m(\mathbf{x}(t_{s-1}))|\mathbf{x}(t_{s-1})]\right], \quad (3)$$

$$\begin{aligned} \mathbb{V}[\hat{x}_m(t_s)] &= \mathbb{V}[\hat{f}_m(\mathbf{x}(t_{s-1}))] \\ &= \mathbb{E}\left[\mathbb{V}[\hat{f}_m(\mathbf{x}(t_{s-1}))|\mathbf{x}(t_{s-1})]\right] + \mathbb{V}\left[\mathbb{E}[\hat{f}_m(\mathbf{x}(t_{s-1}))|\mathbf{x}(t_{s-1})]\right]. \end{aligned} \quad (4)$$

Modeling GPs for  $f_l$  This framework enables the propagation of uncertainties inherent in the inputs through the emulator. Furthermore, the approach has been extended to account for correlated emulators, enabling a comprehensive treatment of dependencies across time steps.

### 3 Fast and exact emulation

In contrast to previously established findings, the prediction of GP with uncertain inputs in the one-step-ahead approach can be made computationally tractable by integrating the concept of Linked GP emulators. To be specific, the proposed approach predicts each state by linking GP outputs recursively, preserving accuracy without the need for sampling. Interestingly, the model structure depicted in Figure 1 can be interpreted as a special case within the emerging field of Deep GP (DGP) models (Damianou and Lawrence, 2013), which have gained significant attention in the computer experiments literature for their hierarchical representation and enhanced flexibility (Sauer et al., 2023; Ming et al., 2023). Unlike canonical DGPs that rely on latent variable hierarchies, the proposed framework employs GP emulators fitted to each state variable, structured in a feed-forward manner reminiscent of deep learning models. This formulation facilitates the propagation of uncertainty across layers while maintaining analytical tractability, thereby enhancing

predictive performance in dynamic system emulation. Building on this integration, we introduce a fast and accurate prediction algorithm for the one-step-ahead approach.

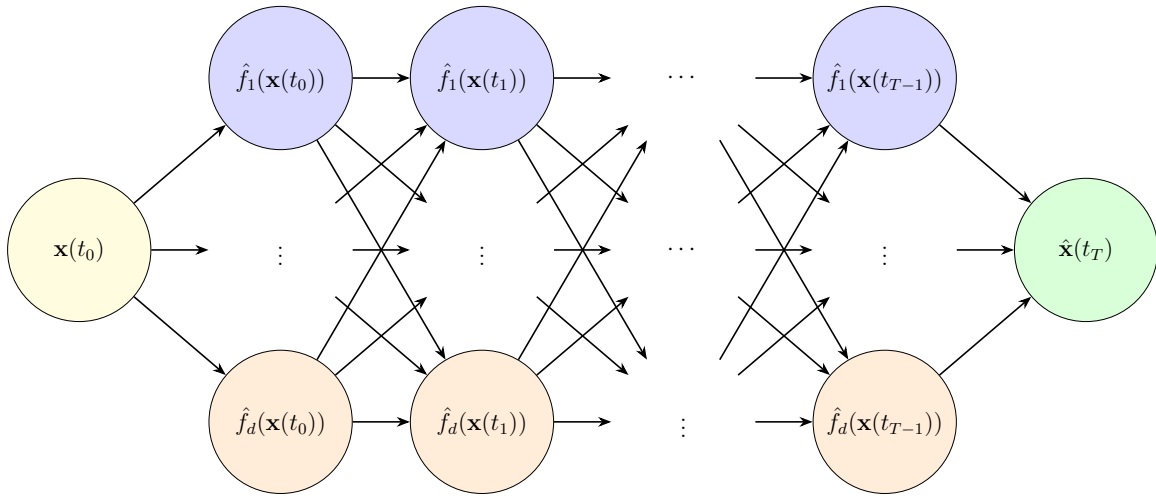


**Figure 1:** An illustration of the self-linked GP emulator for a dynamic system governed by  $d$  ODEs. Starting with the initial state  $\mathbf{x}(t_0)$ , each emulator  $\hat{f}_m$ ,  $m = 1, \dots, d$  predicts the  $m$ -th component of the state  $\hat{x}_m(t_s)$  for  $s = 1, \dots, T$ . The predicted state  $\hat{\mathbf{x}}(t_s)$  is then fed forward as the input for the next time step  $s + 1$ .

### 3.1 Algorithm without forcing inputs

For a nonlinear dynamic simulator  $f$  governed by  $d$  ODEs, consider GP emulators  $\hat{f}_m$ ,  $m = 1, \dots, d$  constructed by using an initial design  $\mathbf{X} = (\mathbf{x}^1(t_0), \dots, \mathbf{x}^n(t_0))$ , and corresponding outputs  $\mathbf{y}_m = (x_m^1(t_1), \dots, x_m^n(t_1))^T$  following the one-step-ahead approach. Instead of relying on MC approximations to compute (3) and (4), we derive analytical expressions for

$\mathbb{E}[\hat{x}_m(t_s)]$  and  $\mathbb{V}[\hat{x}_m(t_s)]$  under the squared exponential kernel given  $\hat{\mathbf{x}}(t_{s-1})$  are as follows:

$$\begin{aligned}\mu_m(\hat{\mathbf{x}}(t_s)) &= \mathbb{E}[\hat{x}_m(t_s)] = \mathbb{E}\left[\hat{f}_m(\hat{\mathbf{x}}(t_{s-1}))\right] \\ &= \left(\mathbf{1} \quad \hat{\mathbf{x}}(t_{s-1})\right) \beta_m + \sum_{i=1}^n r_i \prod_{l=1}^d \sqrt{\frac{\theta_{ml}}{\theta_{ml} + 2\sigma_l^2(\hat{\mathbf{x}}(t_{s-1}))}} \exp\left(-\frac{(x_l^i(t_0) - \mu_l(\hat{\mathbf{x}}(t_{s-1})))^2}{\theta_{ml} + 2\sigma_l^2(\hat{\mathbf{x}}(t_{s-1}))}\right),\end{aligned}\tag{5}$$

and

$$\begin{aligned}\sigma_m^2(\hat{\mathbf{x}}(t_s)) &= \mathbb{V}[\hat{x}_m(t_s)] = \mathbb{V}\left[\hat{f}_m(\hat{\mathbf{x}}(t_{s-1}))\right] \\ &= \tau_m^2 - \left(\mu_m(\hat{\mathbf{x}}(t_s)) - \left(\mathbf{1} \quad \hat{\mathbf{x}}(t_{s-1})\right) \beta_m\right)^2 + \left(\sum_{i,k=1}^n (r_i r_k - \tau_m^2 (\mathbf{K}_m^{-1})_{ik}) \prod_{l=1}^d \zeta_{lik}\right),\end{aligned}\tag{6}$$

where  $r_i = (\mathbf{K}_m^{-1}(\mathbf{y}_m - \mathbf{X}\beta_m))_i$ , and

$$\zeta_{lik} = \sqrt{\frac{\theta_{ml}}{\theta_{ml} + 4\sigma_l^2(\hat{\mathbf{x}}(t_{s-1}))}} \exp\left(-\frac{\left(\frac{x_l^i(t_0) + x_l^k(t_0)}{2} - \mu_l(\hat{\mathbf{x}}(t_{s-1}))\right)^2}{\frac{\theta_{ml}}{2} + 2\sigma_l^2(\hat{\mathbf{x}}(t_{s-1}))} - \frac{(x_l^i(t_0) - x_l^k(t_0))^2}{2\theta_{ml}}\right).$$

The closed-form expressions for the posterior predictive mean (3) and variance (4) under a Matérn kernel with smoothness parameters  $\nu = 1.5$  and  $\nu = 2.5$  can be straightforwardly derived following the proof in Ming and Guillas (2021). Consistent with prior studies (Girard et al., 2002; Kyzuyrova et al., 2018; Mohammadi et al., 2019; Ming and Guillas, 2021), we adopt the moment matching method to approximate the posterior distribution as Gaussian, leveraging the mean and variance from (5) and (6). The moment matching approximation suits the structure of self-linked GP emulator, where outputs recursively

serve as inputs, since the method aligns with the inherent Gaussian nature of GPs and ensures analytical tractability and recursive consistency.

---

**Algorithm 1** Exact emulation of dynamic simulators without forcing inputs

---

```

1: for  $m = 1$  to  $d$  do
2:   Fit  $\hat{f}_m$  using  $\mathbf{X} = (\mathbf{x}^1(t_0), \dots, \mathbf{x}^n(t_0))$ , and  $\mathbf{y}_m = (x_m^1(t_1), \dots, x_m^n(t_1))^T$ 
3: end for
4: Set  $\hat{\mathbf{x}}(t_0) \leftarrow \mathbf{x}(t_0)$ 
5: for  $s = 0$  to  $T - 1$  do
6:   for  $m = 1$  to  $d$  do
7:     Compute  $\mu_m(\hat{\mathbf{x}}(t_{s+1}))$  using (5)
8:     Compute  $\sigma_m^2(\hat{\mathbf{x}}(t_{s+1}))$  using (6)
9:   end for
10:  Update  $s \leftarrow s + 1$ 
11: end for
12: Return:  $\hat{\mathbf{x}}(t_s)$  for  $s = 1, \dots, T$ 

```

---

By leveraging these closed-form expressions, computationally expensive MC approximations can be avoided, allowing for exact computations. The elimination of MC sampling significantly reduces computational costs, making the proposed approach particularly suitable for dynamical systems with many state variables that require extensive simulations. Moreover, the proposed framework provides exact predictive moments, ensuring both efficiency and accuracy. This is particularly advantageous for long-term iterative predictions, where even small numerical errors in early steps can accumulate over time, leading to significant deviations in later steps—a phenomenon often referred to as the *butterfly effect*. By directly computing the mean and variance, our approach mitigates this issue, enhancing robustness in sequential simulations. Furthermore, multi-step-ahead predictions can be efficiently obtained by recursively applying (5) and (6), reducing the need for costly recomputation at each iteration.

### 3.2 Algorithm with forcing input

Assume we have a known,  $d_w$ -dimensional forcing input  $\mathbf{w}(t_s)$  at time  $t_s$  for  $s = 1, \dots, T$ . The dynamic simulator  $f$  can be expressed as:

$$x_m(t_{s+1}) = f_m(\mathbf{x}(t_s), \mathbf{w}(t_s)), \quad \text{for } m = 1, \dots, d. \quad (7)$$

Accordingly, the Markov property must be adjusted to account for forcing inputs. Instead of (2), the emulator follows:

$$\hat{x}_m(t_{s+1}) = \hat{f}_m(\mathbf{x}(t_s), \mathbf{w}(t_s)), \quad (8)$$

where  $m = 1, \dots, d$ . The algorithm proposed in Section 3.1 can be naturally extended to incorporate forcing inputs by treating them as additional variables in the GP framework. This extension preserves the computational efficiency of the method while enabling accurate predictions for systems influenced by external inputs.

To account for forcing inputs, we modify the analytical expressions for  $\mathbb{E}[\hat{x}_m(t_s)]$  and  $\mathbb{V}[\hat{x}_m(t_s)]$  under the squared exponential kernel given  $\hat{\mathbf{x}}(t_{s-1})$  are as follows:

$$\begin{aligned} \mu_m(\hat{\mathbf{x}}(t_s)) &= \left(1 \quad \hat{\mathbf{x}}(t_{s-1})\right) \beta_m \\ &+ \sum_{i=1}^n r_i \prod_{j=1}^{d_w} \exp\left(-\frac{(w_j^i(t_0) - w_j(t_s))^2}{\theta_{wj}}\right) \prod_{l=1}^d \frac{1}{\sqrt{1 + 2\frac{\sigma_l^2(\hat{\mathbf{x}}(t_{s-1}))}{\theta_{ml}}}} \exp\left(-\frac{(x_l^i(t_0) - \mu_l(\hat{\mathbf{x}}(t_{s-1})))^2}{\theta_{ml} + 2\sigma_l^2(\hat{\mathbf{x}}(t_{s-1}))}\right), \end{aligned} \quad (9)$$

and

$$\begin{aligned} \sigma_m^2(\hat{\mathbf{x}}(t_s)) &= \tau_m^2 - \left( \mu_m(\hat{\mathbf{x}}(t_s)) - \left( \mathbf{1} \quad \hat{\mathbf{x}}(t_{s-1}) \right) \beta_m \right)^2 \\ &+ \left( \sum_{i,k=1}^n (r_i r_k - \tau_m^2 (\mathbf{K}_m^{-1})_{ik}) \prod_{j=1}^{d_w} \exp \left( -\frac{(w_j^i(t_0) - (w_j(t_s)))^2 + (w_j^k(t_0) - w_j(t_s))^2}{\theta_{wj}} \right) \prod_{l=1}^d \zeta_{lik} \right), \end{aligned} \quad (10)$$

where  $\theta_{wj}$  for  $j = 1, \dots, d_w$  are the lengthscale hyperparameters associated with the forcing inputs.

---

**Algorithm 2** Exact emulation of dynamic simulators with forcing inputs

---

```

1: for  $m = 1$  to  $d$  do
2:   Fit  $\hat{f}_m$  using  $\mathbf{X} = (\mathbf{x}^1(t_0), \dots, \mathbf{x}^n(t_0))$ ,  $\mathbf{W} = (\mathbf{w}^1(t_0), \dots, \mathbf{w}^n(t_0))$ , and  $\mathbf{y}_m = (x_m^1(t_1), \dots, x_m^n(t_1))^T$ 
3: end for
4: Set  $\hat{\mathbf{x}}(t_0) \leftarrow \mathbf{x}(t_0)$ 
5: for  $s = 0$  to  $T - 1$  do
6:   for  $m = 1$  to  $d$  do
7:     Compute  $\mu_m(\hat{\mathbf{x}}(t_{s+1}))$  using (9) with  $\mathbf{w}(t_s)$ 
8:     Compute  $\sigma_m^2(\hat{\mathbf{x}}(t_{s+1}))$  using (10) with  $\mathbf{w}(t_s)$ 
9:   end for
10:  Update  $s \leftarrow s + 1$ 
11: end for
12: Return:  $\hat{\mathbf{x}}(t_s)$  for  $s = 1, \dots, T$ 

```

---

The additional term in these expressions corresponds to the kernel function  $K(\mathbf{w}(t_0), \mathbf{w}(t_s))$ , which arises because the forcing inputs  $\mathbf{w}(t_s)$  are treated as known rather than random. This assumption simplifies the model structure, as the forcing inputs remain unlinked variables in the emulator.

## 4 Numerical Studies

In this section, we conduct a series of numerical experiments to evaluate the performance of the proposed approach. Specifically, we compare the predictive performance of the proposed exact algorithm with an emulation method based on MC approximation, using  $n_{MC} = 1000$  samples. Both approaches employ the same GP emulator, using an anisotropic squared exponential kernel and a linear mean function  $\alpha(\mathbf{x}) = (1, \mathbf{x}^T)\beta$ .

All numerical studies are conducted using a maximin Latin hypercube design (Johnson et al., 1990; Morris and Mitchell, 1995), with the number of initial samples set to  $n = 12d$ , following the guidelines of Mohammadi et al. (2019), which builds on the design principles established in Jones et al. (1998) and Loepky et al. (2009). The time step difference is set to  $\Delta t = t_s - t_{s-1} = 0.01$ .

The governing ODEs of the dynamic simulators are solved using the `lsoda` method from the R package `deSolve` (Soetaert et al., 2010). This solver, known as the Livermore solver for stiff and non-stiff ODE systems, automatically switches between stiff and non-stiff methods for efficiency (Petzold, 1983).

To evaluate predictive performance, we compute predictions at all time points  $t_s$ ,  $s = 1, \dots, T$ , and assess model accuracy using the root-mean-square error (RMSE) and continuous rank probability score (CRPS) (Gneiting and Raftery, 2007) over 100 repetitions. The evaluation metrics are defined as follows:

$$\text{RMSE} = \sqrt{\sum_{i=1}^n \frac{(y_i - \hat{y}_i)^2}{n}},$$

$$\text{CRPS} = \sigma \left[ \frac{1}{\sqrt{\pi}} - 2\phi\left(\frac{y - \mu}{\sigma}\right) - \frac{y - \mu}{\sigma} \left( 2\Phi\left(\frac{y - \mu}{\sigma}\right) - 1 \right) \right],$$

where  $y$  represents the true function values,  $\mu$  and  $\sigma^2$  denote the posterior predictive

mean and variance, respectively.  $\phi$  and  $\Phi$  are the pdf and the cdf of a standard Gaussian distribution. These metrics quantify the degree of discrepancy between the true function and the predictive model, with lower RMSE and CRPS values indicating better model accuracy. Furthermore, we evaluate computational efficiency by comparing computation times across different emulation approaches.

## 4.1 Lotka-Volterra model

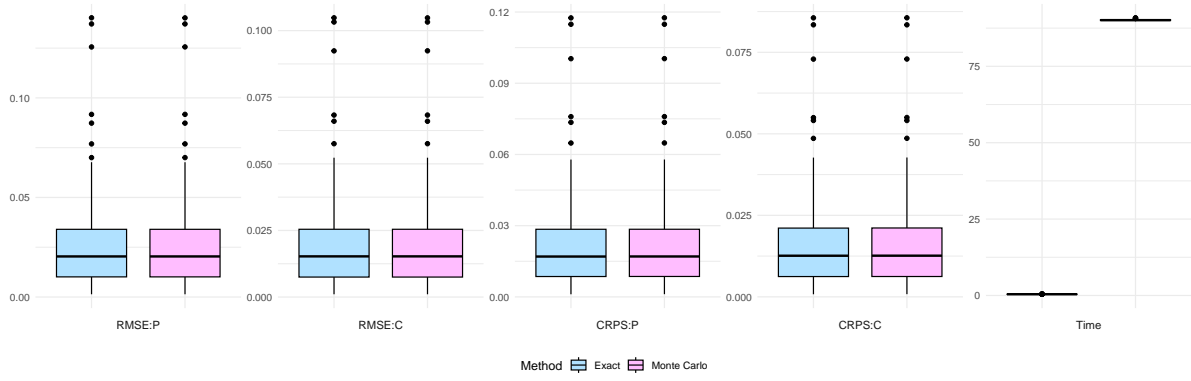
The Lotka-Volterra model (Lotka, 1925; Volterra, 1927; Goel et al., 1971), also known as the consumer-prey model, is a foundational framework in mathematical ecology for describing predator-prey dynamics. This model characterizes the temporal evolution of two interacting populations: a prey species with population density  $P(t)$  and a predator species with population density  $C(t)$ . The dynamics are governed by the following system of nonlinear differential equations:

$$\begin{cases} \frac{dP}{dt} &= r_G \cdot P \cdot \left(1 - \frac{P}{K}\right) - r_I \cdot P \cdot C, \\ \frac{dC}{dt} &= k_{AE} \cdot r_I \cdot P \cdot C - r_M \cdot C, \end{cases}$$

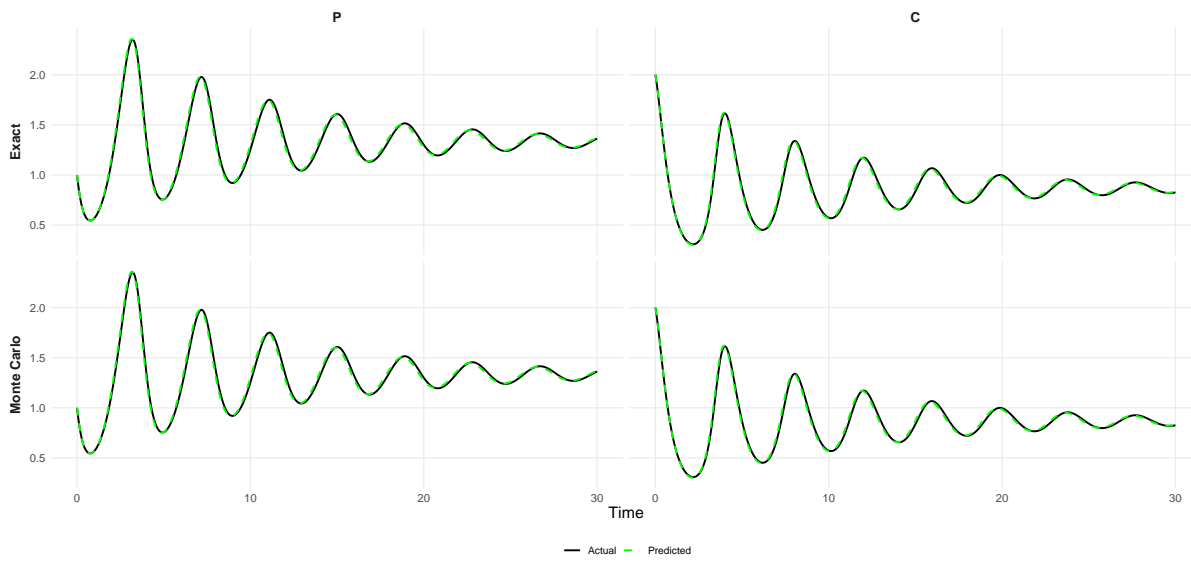
where  $r_G > 0$  represents the intrinsic growth rate of the prey in the absence of predators,  $K$  is the prey carrying capacity,  $r_I > 0$  is the predation rate coefficient,  $k_{AE} > 0$  is the assimilation efficiency of the predator, and  $r_M > 0$  denotes the natural mortality rate of the predator in the absence of prey. For this study, we consider a simulation over  $t \in [0, 30]$ , with prespecified parameter values  $r_G = 1.5$ ,  $K = 10$ ,  $r_I = 1.5$ ,  $k_{AE} = 1$ , and  $r_M = 2$ . Initial samples are drawn from  $[0, 5]^2$ . The objective is to predict the system's dynamics given the initial state  $\mathbf{x}(t_0) = (P(t_0) = 1, C(t_0) = 2)$ .

Figure 2 presents the emulation results over 100 repetitions for RMSE and CRPS, while





**Figure 2:** *RMSE (first and second plots), CRPS (third and fourth plots) of emulation algorithms to P and C and computation time (fifth plots) across 100 repetitions for Lotka-Volterra model.*



**Figure 3:** *Lotka-Volterra model (black solid line) and emulation results of prediction (green dashed line) via each algorithm.*

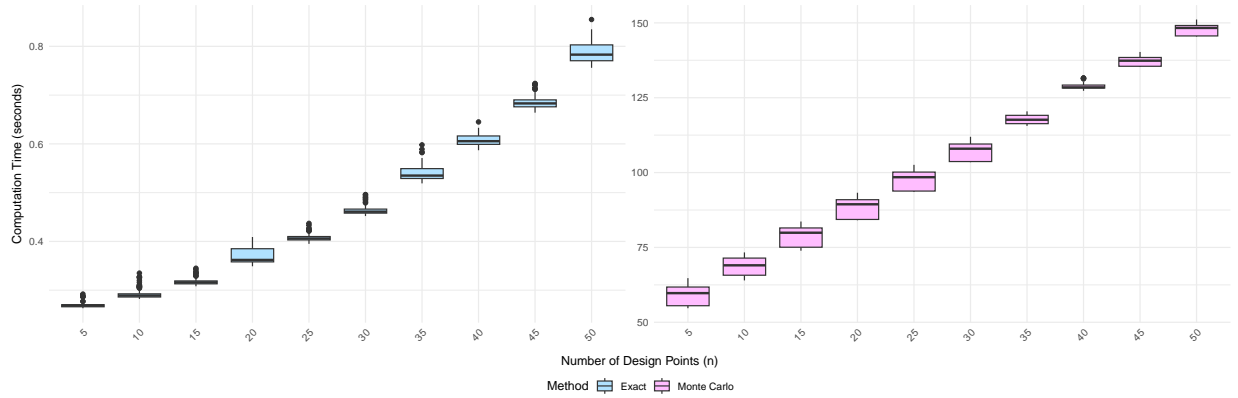


**Figure 4:** *Boxplots of computation time for the Exact and Monte Carlo methods as the number of design points varies from 5 to 50 in increments of 5 across 100 repetitions for Lotka-Volterra model.*

Figure 3 illustrates the predicted trajectories for state variables,  $P$  and  $C$ , respectively. As expected, both algorithms produce nearly identical predictions, with a maximum difference of only 0.000024. While both methods achieve high predictive accuracy, their computational costs differ considerably. On average, the exact algorithm requires only 0.40603 seconds per repetition, whereas the MC approach takes 90.13912 seconds. This comparison highlights the advantage of the proposed framework in significantly reducing computational cost while maintaining accuracy in dynamic system emulation. Moreover, the computational gap would increase further if the MC approach employed a larger number of samples, or if the simulation involved many time steps or a longer time horizon.

Figure 4 illustrates the computation time for emulation as the number of samples varies from 5 to 50 per repetition. With a precomputed  $\mathbf{K}^{-1}$ , the computational complexity of computing the predictive mean and variance at a single input location using MC-based emulation is  $\mathcal{O}(n^2 n_{MC})$ . On the other hand, under the same conditions, the exact algorithm requires only  $\mathcal{O}(n^2 d)$  complexity. Since  $n_{MC}$  is typically in the range of several thousand or

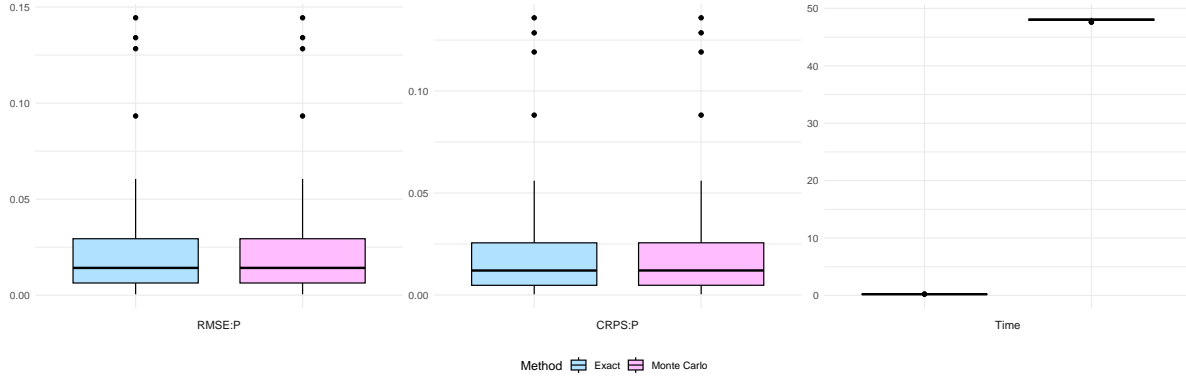


**Figure 5:** *RMSE (first plot), CRPS (second plot) of emulation algorithms to  $P$  with forcing input  $C$  and computation time (third plot) across 100 repetitions for Lotka-Volterra model.*

more, the proposed algorithm offers substantial computational savings.

Figure 5 demonstrates the results for the case in which  $C(t)$  is treated as a forcing input. As anticipated, the emulation performance improves due to the availability of a known input, and the computation time is halved with 0.20403 seconds per repetition for the exact algorithm and 48.03827 seconds for the MC-based algorithm. These results confirm that the exact method remains computationally efficient in the presence of a forcing input.

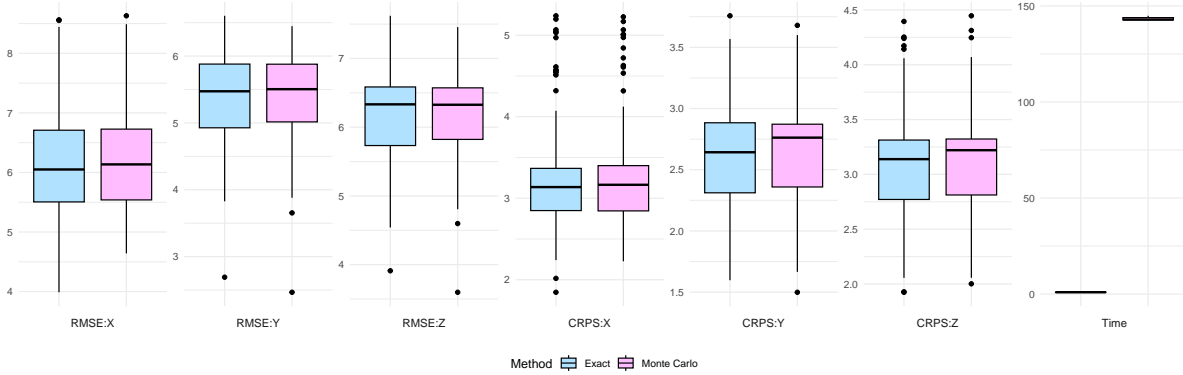


**Figure 6:** *RMSE (first to third plots), CRPS (fourth to sixth plots) of emulation algorithms to  $P$  and  $C$  and computation time (seventh plots) across 100 repetitions for Lorenz system.*

## 4.2 Lorenz system

The Lorenz system, introduced by Lorenz (1963), models the behavior of atmospheric convection through a set of three differential equations:

$$\begin{cases} \frac{dX}{dt} = aX + YZ, \\ \frac{dY}{dt} = b(Y - Z), \\ \frac{dZ}{dt} = -XY + cY - Z, \end{cases}$$

where  $X$ ,  $Y$ , and  $Z$  represent the system's state variables, and  $a$ ,  $b$ , and  $c$  are system parameters that govern the system's dynamics. Using the classic values  $a = -8/3$ ,  $b = -10$ , and  $c = 28$ , originally employed by Lorenz to study convection rolls, the system exhibits chaotic behavior. We focus on a simulation over  $t \in [0, 25]$ , and the initial state  $\mathbf{x}(t_0) = (X(t_0) = -1, Y(t_0) = -1, Z(t_0) = -1)$ . Initial designs are sampled from  $[-10, 10]^3$ .

From Figure 6, the emulation results show slight differences between the two algorithms.

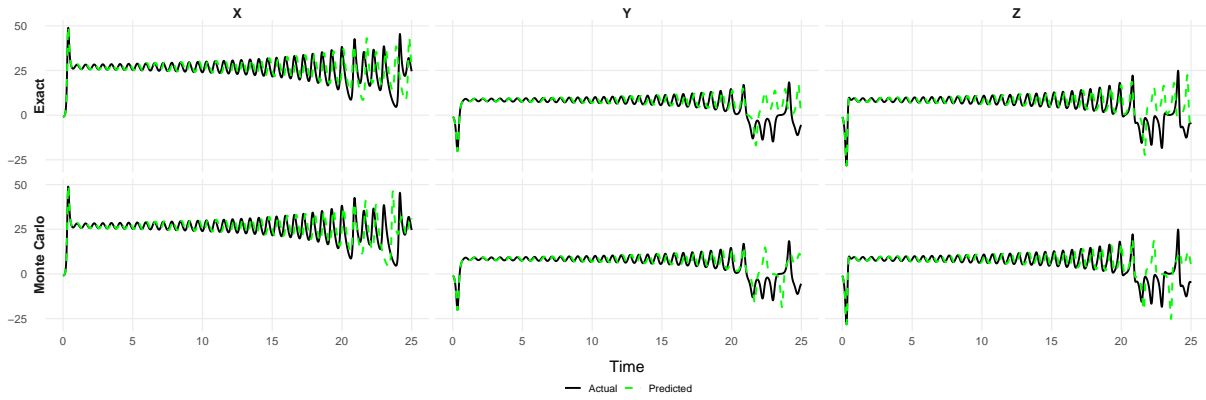


**Figure 7:** Lorenz system (black solid line) and emulation results of prediction (green dashed line) via each algorithm.

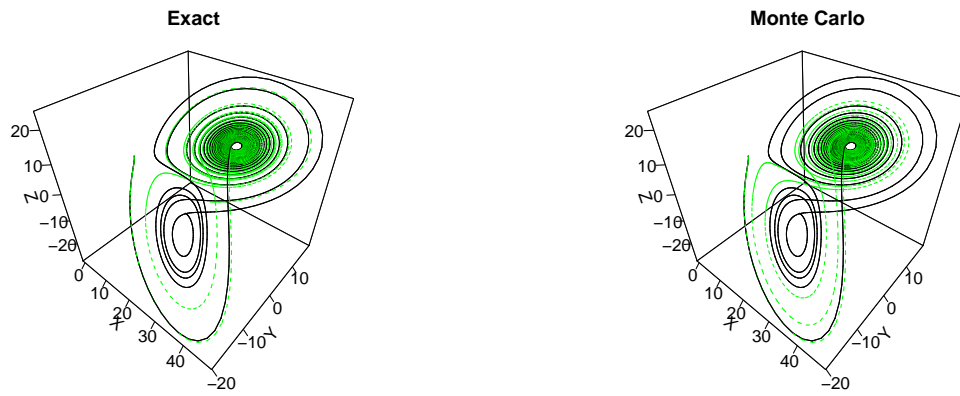


**Figure 8:** 3-d illustrations of Lorenz system (black solid line) and emulation results of prediction (green dashed line) via each algorithm.

This discrepancy arises because the Lorenz system is highly sensitive to small changes, which can lead to significant differences, a phenomenon known as the “butterfly effect”.

As shown, the exact algorithm can emulate the system efficiently, requiring only 0.95777 seconds per repetition, whereas the MC approach takes significantly longer at 143.22403 seconds. Figures 7 and 8 illustrate the predicted trajectories for each state variable,  $X$ ,  $Y$ , and  $Z$ . Both algorithms provide accurate predictions at early time steps up to  $t = 20$ , but their performance deteriorates beyond this point. For highly sensitive dynamic systems such as the Lorenz system, the exact algorithm is particularly advantageous, as MC methods introduce variations that exacerbate prediction errors over time. This underscores the importance of exact emulation for improving accuracy and computational efficiency in chaotic systems.

## 5 Discussion

In this paper, we propose fast and exact algorithms for emulating complex dynamic simulators. These algorithms enable efficient emulation compared to traditional MC-based approaches, while retaining their advantages. Numerical studies demonstrate that our method achieves equivalent results with significantly reduced computation time, over 100 times faster. Additionally, our approach accurately computes the predictive posterior mean and variance, preventing the accumulation of small differences from sampling errors.

From a computational perspective, the addition of jitter for numerical stability—commonly used to avoid ill-conditioned covariance matrices—may introduce minor discrepancies that could accumulate over time. In dynamic systems that are highly sensitive to small changes, such as those exhibiting the butterfly effect, these numerical artifacts can significantly impact the emulation outcomes. Furthermore, computational efficiency can be further improved by implementing low-level programming languages for operations.

In this work, although the state variables are correlated, we followed the approach of

Damianou and Lawrence (2013) and independently constructed the emulators. However, as suggested by Mohammadi et al. (2019), neglecting these correlations might lead to information loss, potentially affecting predictive accuracy. Future work could address this limitation by incorporating correlations among state variables, further enhancing emulation performance.

Another promising direction for future research lies in the emulation of non-periodic chaotic systems, such as the three-body problem (Newton, 1687; Musielak and Quarles, 2014). Chaotic systems are inherently unpredictable and highly sensitive to initial conditions, making them particularly challenging to emulate. To enhance model accuracy in such cases, integrating active learning, where new training points are adaptively selected to improve emulation performance could be a valuable approach for dynamic system emulation.

## References

- Bahamonde, S., Böhmer, C. G., Carloni, S., Copeland, E. J., Fang, W., and Tamanini, N. (2018). Dynamical systems applied to cosmology: dark energy and modified gravity. *Physics Reports*, 775:1–122.
- Bhattacharya, S. (2007). A simulation approach to bayesian emulation of complex dynamic computer models. *Bayesian Analysis*, 2(4):783–815.
- Bongard, J. and Lipson, H. (2007). Automated reverse engineering of nonlinear dynamical systems. *Proceedings of the National Academy of Sciences*, 104(24):9943–9948.
- Byrd, R. H., Lu, P., Nocedal, J., and Zhu, C. (1995). A limited memory algorithm for bound constrained optimization. *SIAM Journal on scientific computing*, 16(5):1190–1208.

- Conti, S., Gosling, J. P., Oakley, J. E., and O’Hagan, A. (2009). Gaussian process emulation of dynamic computer codes. *Biometrika*, 96(3):663–676.
- Damianou, A. and Lawrence, N. D. (2013). Deep Gaussian processes. In *Artificial Intelligence and Statistics*, pages 207–215. PMLR.
- Dolski, T., Spiller, E. T., and Minkoff, S. E. (2024). Gaussian process emulation for high-dimensional coupled systems. *Technometrics*, 66(3):455–469.
- Girard, A., Rasmussen, C., Candela, J. Q., and Murray-Smith, R. (2002). Gaussian process priors with uncertain inputs application to multiple-step ahead time series forecasting. *Advances in neural information processing systems*, 15.
- Gneiting, T. and Raftery, A. E. (2007). Strictly proper scoring rules, prediction, and estimation. *Journal of the American Statistical Association*, 102(477):359–378.
- Goel, N. S., Maitra, S. C., and Montroll, E. W. (1971). On the volterra and other nonlinear models of interacting populations. *Reviews of modern physics*, 43(2):231.
- Gramacy, R. B. (2020). *Surrogates: Gaussian Process Modeling, Design, and Optimization for the Applied Sciences*. CRC press.
- Heo, J. and Sung, C.-L. (2023). Active learning for a recursive non-additive emulator for multi-fidelity computer experiments. *arXiv preprint arXiv:2309.11772*.
- Hwang, Y., Kim, H. J., Chang, W., Hong, C., and MacEachern, S. N. (2025). Bayesian model calibration and sensitivity analysis for oscillating biological experiments. *Technometrics*, pages 1–11.



- Johnson, M. E., Moore, L. M., and Ylvisaker, D. (1990). Minimax and maximin distance designs. *Journal of statistical planning and inference*, 26(2):131–148.
- Jones, D. R., Schonlau, M., and Welch, W. J. (1998). Efficient global optimization of expensive black-box functions. *Journal of Global optimization*, 13:455–492.
- Kyzyurova, K. N., Berger, J. O., and Wolpert, R. L. (2018). Coupling computer models through linking their statistical emulators. *SIAM/ASA Journal on Uncertainty Quantification*, 6(3):1151–1171.
- Li, J., Li, G., Xu, J., Dong, P., Qiao, L., Liu, S., Sun, P., and Fan, Z. (2016). Seasonal evolution of the yellow sea cold water mass and its interactions with ambient hydrodynamic system. *Journal of Geophysical Research: Oceans*, 121(9):6779–6792.
- Loeppky, J. L., Sacks, J., and Welch, W. J. (2009). Choosing the sample size of a computer experiment: A practical guide. *Technometrics*, 51(4):366–376.
- Lorenz, E. N. (1963). Deterministic nonperiodic flow. *Journal of the Atmospheric Sciences*, 20(2):130–141.
- Lotka, A. J. (1925). *Elements of physical biology*. Williams & Wilkins.
- Millán, H., Kalauzi, A., Llerena, G., Sucoshañay, J., and Piedra, D. (2009). Meteorological complexity in the amazonian area of ecuador: An approach based on dynamical system theory. *Ecological Complexity*, 6(3):278–285.
- Ming, D. and Guillas, S. (2021). Linked Gaussian process emulation for systems of computer models using Matérn kernels and adaptive design. *SIAM/ASA Journal on Uncertainty Quantification*, 9(4):1615–1642.

- Ming, D., Williamson, D., and Guillas, S. (2023). Deep Gaussian process emulation using stochastic imputation. *Technometrics*, 65(2):150–161.
- Mohammadi, H., Challenor, P., and Goodfellow, M. (2019). Emulating dynamic non-linear simulators using gaussian processes. *Computational Statistics & Data Analysis*, 139:178–196.
- Mohammadi, H., Challenor, P., and Goodfellow, M. (2024). Emulating complex dynamical simulators with random fourier features. *SIAM/ASA Journal on Uncertainty Quantification*, 12(3):788–811.
- Morris, M. D. and Mitchell, T. J. (1995). Exploratory designs for computational experiments. *Journal of statistical planning and inference*, 43(3):381–402.
- Musielak, Z. E. and Quarles, B. (2014). The three-body problem. *Reports on Progress in Physics*, 77(6):065901.
- Newton, I. (1687). *Philosophiae naturalis principia mathematica*. London: Royal Society Press.
- Petzold, L. (1983). Automatic selection of methods for solving stiff and nonstiff systems of ordinary differential equations. *SIAM journal on scientific and statistical computing*, 4(1):136–148.
- Rasmussen, C. E. and Williams, C. K. (2006). *Gaussian Processes for Machine Learning*. Cambridge, MA: MIT Press.
- Santner, T. J., Williams, B. J., and Notz, W. I. (2018). *The Design and Analysis of Computer Experiments*. Springer New York.

- Sauer, A., Gramacy, R. B., and Higdon, D. (2023). Active learning for deep Gaussian process surrogates. *Technometrics*, 65(1):4–18.
- Scheinerman, E. R. (2012). *Invitation to dynamical systems*. Courier Corporation.
- Soetaert, K. E., Petzoldt, T., and Setzer, R. W. (2010). Solving differential equations in r: package desolve. *Journal of statistical software*, 33(9).
- Stein, M. L. (1999). *Interpolation of Spatial Data: Some Theory for Kriging*. Springer Science & Business Media.
- Stolfi, P. and Castiglione, F. (2021). Emulating complex simulations by machine learning methods. *BMC Bioinformatics*, 22:1–14.
- Volterra, V. (1927). Fluctuations in the abundance of a species considered mathematically. *Nature*, 119(2983):12–13.
- Zhu, C., Byrd, R. H., Lu, P., and Nocedal, J. (1997). Algorithm 778: L-bfgs-b: Fortran subroutines for large-scale bound-constrained optimization. *ACM Transactions on mathematical software (TOMS)*, 23(4):550–560.